



PII S0016-7037(99)00217-3

Effects of growth rate, CO₂ concentration, and cell size on the stable carbon isotope fractionation in marine phytoplankton

STEFFEN BURKHARDT,* ULF RIEBESELL, and INGRID ZONDERVAN

Alfred Wegener Institute for Polar and Marine Research, Am Handelshafen 12, D-27570 Bremerhaven, Germany

(Received December 14, 1998; accepted in revised form June 7, 1999)

Abstract—Stable carbon isotope fractionation (ϵ_p) was measured in four marine diatom and one dinoflagellate species of different cell sizes. Monospecific cultures were incubated under high-light and nutrient-replete conditions at 16 h : 8 h and 24 h : 0 h light/dark cycles in dilute batch cultures at six CO₂ concentrations, [CO_{2, aq}], ranging from ca. 1 to 38 $\mu\text{mol kg}^{-1}$. In all species, ϵ_p increased with increasing [CO_{2, aq}]. Among the diatoms, the degree of CO₂-related variability in ϵ_p was inversely correlated with cell size. Isotopic fractionation in the dinoflagellate differed in several aspects from that of the diatoms, which may reflect both morphological and physiological differences between taxa. Daylength-related changes in instantaneous growth rate, defined as the rate of C assimilation during the photoperiod, affected ϵ_p to a similar or greater extent than differences in experimental [CO_{2, aq}] in three of the species tested. In contrast, the irradiance cycle had no effect on ϵ_p in 2 other species. With the exception of *Phaeodactylum tricornutum*, growth rate of all species declined below a critical [CO_{2, aq}]. At these concentrations, we observed a reversal in the CO₂-related ϵ_p trend, which we attribute to a decline in carbon assimilation efficiency. Although uncatalyzed passive diffusion of CO₂ into the cell was sufficient to account for gross carbon uptake in most treatments, our results indicate that other processes contribute to inorganic carbon acquisition in all species even at [CO_{2, aq}] > 10 $\mu\text{mol kg}^{-1}$. These processes may include active C transport and/or catalyzed conversion of HCO₃⁻ to CO₂ by carbonic anhydrase. A comparison of our results with data from the literature indicates significant deviations from previously reported correlations between ϵ_p and μ /[CO_{2, aq}], even when differences in cellular carbon content and cell geometry are accounted for. Copyright © 1999 Elsevier Science Ltd

1. INTRODUCTION

During photosynthetic fixation of CO₂ into organic material, algal cells discriminate against the heavier stable carbon isotope ¹³C. As a result of this fractionation process, marine phytoplankton are depleted in ¹³C relative to the inorganic carbon source. Variations in the isotopic composition ($\delta^{13}\text{C}$) of sedimentary organic carbon have been correlated with concentrations of molecular dissolved CO₂, [CO_{2, aq}], in surface water (Rau et al., 1989, 1992) with marine plankton being most depleted in ¹³C at high latitudes (Sackett et al., 1965; Rau et al., 1982, 1989). This led to the suggestion that isotope measurements of sedimentary organic matter may be used for the reconstruction of ancient CO₂ concentrations in ocean surface waters (e.g., Freeman and Hayes, 1992; Jasper et al., 1994; Rau, 1994).

Factors other than CO₂, however, may also have a significant impact on the isotopic composition in microalgae. Algal growth rate (μ) is a key variable in the fractionation process and isotopic fractionation in mixed phytoplankton assemblages can be influenced by taxon-specific differences (e.g., Francois et al., 1993; Goericke et al., 1994; Laws et al., 1995; Rau et al., 1996; Popp et al., 1998). Furthermore, the nutritional status of the cells may affect isotope fractionation (Kukert and Riebesell, 1998).

An inverse correlation is predicted for ϵ_p as a function of μ /[CO_{2, aq}] (Francois et al., 1993; Laws et al., 1995, 1997; Rau et al., 1996). At CO₂ concentrations exceeding 10 $\mu\text{mol kg}^{-1}$,

linearity of this relationship has been demonstrated for the diatoms *Phaeodactylum tricornutum* (Laws et al., 1995), *Porosira glacialis* (Popp et al., 1998), and for the coccolithophorid *Emiliania huxleyi* (Bidigare et al., 1997). Differences in the slopes of ϵ_p vs. μ /[CO_{2, aq}] regression lines between these species could be accounted for by differences in the surface area and cellular carbon content (Popp et al., 1998). These results are consistent with (but do not prove) CO₂ being the carbon species entering the cell. It is important to keep in mind that one cannot distinguish between CO₂ and HCO₃⁻ uptake in algal cells based on isotope data alone, if they are not accompanied by additional information (Laws et al., 1997; Keller and Morel, 1999).

Regardless of the carbon acquisition mechanism, Popp et al. (1998) conclude that the empirical relationship between ϵ_p and μ /[CO_{2, aq}] may be used to determine paleo-[CO_{2, aq}], when growth rates, cell size, and geometry can be constrained. Alternatively, in situ growth rates of phytoplankton could be estimated from ϵ_p , [CO_{2, aq}], cell size, and geometry. The authors point out, however, that “further studies are required to clearly separate the effects of growth rate, cell geometry, and [CO_{2, aq}] on ϵ_p .” We feel that more species need to be tested to provide a larger database for calibration. Furthermore, the reported empirical relationship relies exclusively on laboratory experiments performed under nitrogen-limited conditions in continuous culture. If a regulated transport mechanism is involved in inorganic carbon acquisition, μ -related variability in ϵ_p might depend on the factor controlling growth rate. Finally, growth rate and [CO_{2, aq}] were manipulated simultaneously in the above-mentioned experiments so that the relative contribu-

* Author to whom correspondence should be addressed (sburkhardt@awi-bremerhaven.de).

tion of each of these factors to changes in ε_p could not be quantified.

Our experiments were intended to: (1) determine the ε_p vs. $\mu/[\text{CO}_{2,\text{aq}}]$ relationship in several species of marine microalgae; (2) avoid colimitation of algal growth by $[\text{CO}_{2,\text{aq}}]$ and nutrient supply or light intensity during the experiments; and (3) distinguish between the relative impact of variation in $[\text{CO}_{2,\text{aq}}]$ and growth rate on ε_p . For that purpose, we investigated stable carbon isotope fractionation in the marine diatoms *Asterionella glacialis*, *Thalassiosira punctigera*, *Coscinodiscus wailesii*, *Phaeodactylum tricorutum*, and in the dinoflagellate *Scrippsiella trochoidea* under high-light, nutrient-replete conditions in dilute batch cultures. Dependence of both ε_p and μ on $[\text{CO}_{2,\text{aq}}]$ in each species was evaluated at six CO_2 concentrations, ranging from ca. 1 to 38 $\mu\text{mol kg}^{-1}$. In addition, the algae were cultivated under two irradiance cycles in order to vary growth rate independent of $[\text{CO}_{2,\text{aq}}]$ at each of the different CO_2 levels. With this approach, we can separate the effect of growth rate on isotopic fractionation from CO_2 -related effects. Furthermore, we use our data to test the applicability of the published ε_p vs. $\mu/[\text{CO}_{2,\text{aq}}]$ regressions to phytoplankton growth under nutrient-replete conditions. Finally, we consider the effect of cellular carbon content and surface area on ε_p in the five species, which covered a wide range in cell size.

The following terminology is used in this article. "Carbon supply" refers to the flux of inorganic carbon to the outer surface of an algal cell. "Carbon uptake" describes the transport of inorganic carbon through the plasmalemma into the cell, either by passive diffusion or by an active transport mechanism. "Carbon acquisition" involves both carbon uptake and subsequent transport of inorganic carbon across the chloroplast envelope to the sites of carbon fixation. Furthermore, production of extracellular carbonic anhydrase, which catalyzes the conversion of HCO_3^- to CO_2 at the outer cell surface, is regarded as a carbon acquisition mechanism. "Carbon fixation" is the incorporation of inorganic carbon into organic carbon compounds.

2. MATERIAL AND METHODS

With the exception of *P. tricorutum* (strain CCAP 1052/1A), all species tested were grown from recent isolates from the southern North Sea. In all treatments, cells were incubated at 15°C in 16 h : 8 h or 24 h : 0 h light/dark cycles at a photon flux density of 150 $\mu\text{mol photons m}^{-2} \text{s}^{-1}$ (400–700 nm radiation) and nutrient concentrations of 100 $\mu\text{mol kg}^{-1}$ nitrate, 100 $\mu\text{mol kg}^{-1}$ silicate, and 6.25 $\mu\text{mol kg}^{-1}$ phosphate. Trace metals and vitamins were added according to f/2 enrichment (Guillard and Ryther, 1962). For each species, six different CO_2 concentrations between ca. 1 and 38 $\mu\text{mol kg}^{-1}$ were adjusted by variation of pH between 9.1 and 7.8 upon the addition of HCl or NaOH at a constant concentration of dissolved inorganic carbon (DIC). This range in pH is identical to the variation in pH that would accompany corresponding changes in CO_2 concentration in the ocean or in aerated experimental systems (e.g., Laws et al., 1995, 1997).

All experiments were performed in 2.4-L dilute batch cultures, which were typically harvested at 20–30 $\mu\text{mol kg}^{-1}$ particulate organic carbon (POC) and never exceeded 50 $\mu\text{mol kg}^{-1}$ POC final concentration. In contrast to chemostat cultures, cells thus grew under nutrient-replete conditions at low maximum cell densities, which were of the same magnitude as can be encountered under bloom conditions in the field. In our dilute cultures, changes in pH during incubation were always <0.05 and changes in the isotopic composition of DIC never exceeded 0.4‰. Precision of the measurements was $\pm 1 \mu\text{mol kg}^{-1}$ (DIC), $\pm 5 \mu\text{eq kg}^{-1}$ (total alkalinity), $\pm 0.1\text{‰}$ ($\delta^{13}\text{C}_{\text{DIC}}$), $\pm 0.3\text{‰}$ ($\delta^{13}\text{C}_{\text{POC}}$). For further details on methods and experimental protocol,

we refer to Burkhardt et al. (1999). In the following, we briefly summarize how the key parameters relevant to our data interpretation were determined.

Concentrations of CO_2 were calculated from DIC, total alkalinity, temperature, salinity, and concentrations of silicate and phosphate assuming dissociation constants of Mehrbach et al. (1973). The isotopic composition of CO_2 ($\delta^{13}\text{C}_{\text{CO}_2}$) was determined from $\delta^{13}\text{C}_{\text{DIC}}$ and absolute temperature (T_k , in Kelvin) according to Mook et al. (1974) by using the equation provided by Rau et al. (1996):

$$\delta^{13}\text{C}_{\text{CO}_2} = \delta^{13}\text{C}_{\text{DIC}} + 23.644 - \frac{9701.5}{T_k} \quad (1)$$

Isotopic fractionation was calculated relative to CO_2 as a carbon source according to Freeman and Hayes (1992):

$$\varepsilon_p = \frac{\delta^{13}\text{C}_{\text{CO}_2} - \delta^{13}\text{C}_{\text{POC}}}{1 + \delta^{13}\text{C}_{\text{POC}}/1000} \quad (2)$$

The average 24-h growth rate μ_{L+D} was estimated from changes in concentrations of particulate organic carbon from $[\text{POC}]_i$ to $[\text{POC}]_{i+1}$ over the time interval t_i to t_{i+1} :

$$\mu_{L+D} = \frac{\ln[\text{POC}]_{i+1} - \ln[\text{POC}]_i}{t_{i+1} - t_i} \quad (3)$$

Two-point measurements of growth rates on a cellular basis between the beginning and the end of incubation were compared to daily cell counts in control bottles to examine whether a prolonged lag phase affected growth rate estimates (Burkhardt et al., 1999). No significant differences in growth rate were detected between calculation from daily cell counts and two-point measurements based on cell counts or POC measurements. Because isotopic fractionation occurs mainly by enzymatic fixation of CO_2 during photosynthesis, we calculated the instantaneous rate of growth (μ_i) from μ_{L+D} by accounting for the light phase (L), the dark phase (D), and dark carbon loss (r):

$$\mu_i = \frac{(L + D)\mu_{L+D}}{L - D r} \quad (4)$$

Because we did not measure dark carbon loss in our experiments, we assumed its rate to equal 15% of the rate of carbon assimilation during the preceding photoperiod (Laws and Bannister, 1980) in which case r equals 0.15 in Eqn. 4.

3. EXPERIMENTAL RESULTS

Species-specific differences in both the dependence of μ_i on $[\text{CO}_{2,\text{aq}}]$ and the relationship of ε_p with $[\text{CO}_{2,\text{aq}}]$, μ_i , and $\mu_i/[\text{CO}_{2,\text{aq}}]$ were found over the entire experimental CO_2 range (Figs. 1 to 5). We observed a significant decrease in μ_i at $[\text{CO}_{2,\text{aq}}] \leq \text{ca. } 3 \text{ to } 6 \mu\text{mol kg}^{-1}$ in all species except for *P. tricorutum*, which exhibited constant growth rates over the entire $[\text{CO}_{2,\text{aq}}]$ range from 2.1 to 38 $\mu\text{mol kg}^{-1}$. In all species, μ_i was approximately 50 to 70% higher in a 16 h : 8 h L/D cycle compared to growth under continuous light.

Above the CO_2 threshold concentration C_{lim} , defined as the concentration below which growth rate is CO_2 -dependent, isotopic fractionation increased with increasing $[\text{CO}_{2,\text{aq}}]$ in all species tested (Figs. 1b–5b). Only in *C. wailesii* did we observe little or no increase in ε_p even at the highest CO_2 concentration when grown in a 16 h : 8 h L/D cycle. Absolute values of ε_p tended to be smaller in large cells at a given CO_2 concentration. In all diatoms except *P. tricorutum*, CO_2 -related effects on ε_p were greater when cells grew under continuous light. *S. trochoidea* was the only species in which isotopic fractionation assumed values near zero at low $[\text{CO}_{2,\text{aq}}]$.

At or below C_{lim} , ε_p values no longer decreased with decreasing $[\text{CO}_{2,\text{aq}}]$ but remained constant or increased. Such a

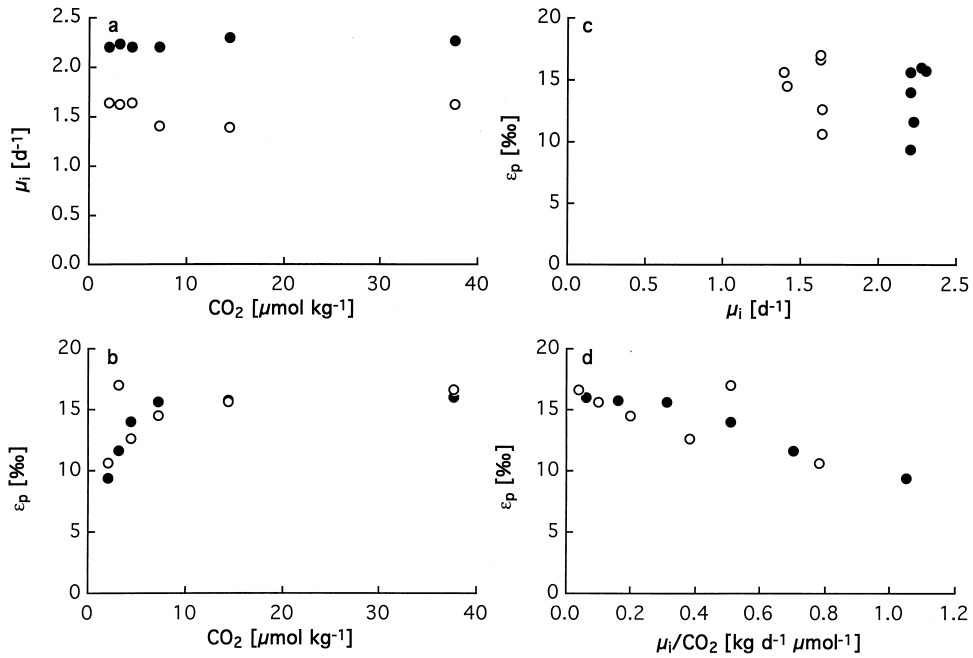


Fig. 1. *Phaeodactylum tricornutum*. (a) Instantaneous growth rate (μ_i) as a function of $[\text{CO}_{2,\text{aq}}]$, and stable carbon isotope fractionation as a function of (b) $[\text{CO}_{2,\text{aq}}]$, (c) μ_i , and (d) $\mu_i/[\text{CO}_{2,\text{aq}}]$. Full symbols and open symbols represent incubation at a 16 h : 8 h L/D cycle and continuous light, respectively.

reversal in the CO_2 -related ϵ_p trend was most pronounced in the largest species (*T. punctigera* and *C. wailesii*). In *P. tricornutum*, where μ_i was independent of $[\text{CO}_{2,\text{aq}}]$ over the entire

experimental range, ϵ_p continuously decreased toward the lowest $[\text{CO}_{2,\text{aq}}]$ in both irradiance cycles.

We observed a decrease in ϵ_p with increasing μ_i in *T.*

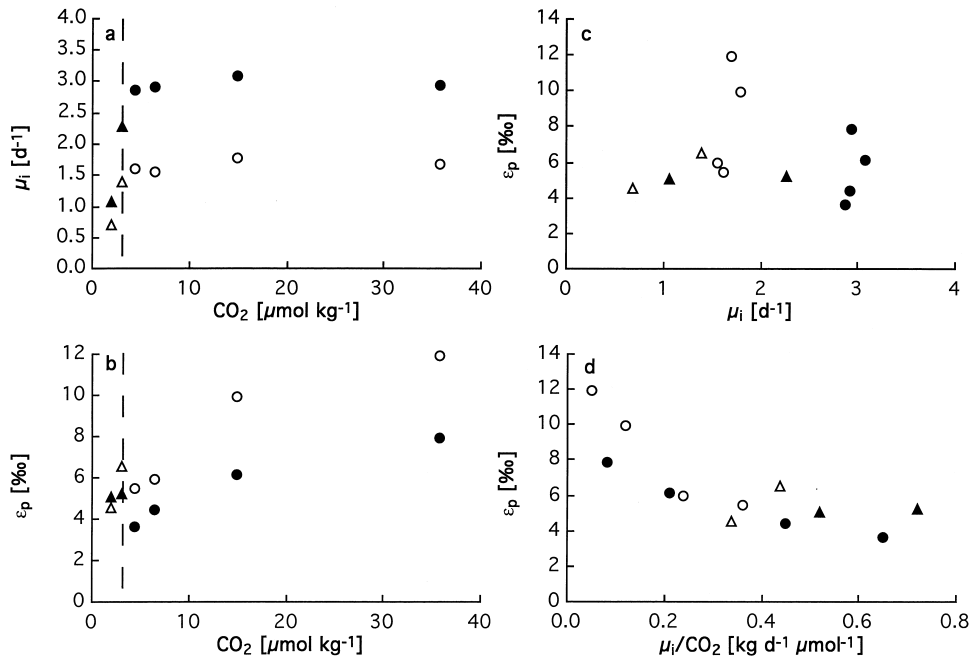


Fig. 2. *Asterionella glacialis*. (a) Instantaneous growth rate (μ_i) as a function of $[\text{CO}_{2,\text{aq}}]$ and stable carbon isotope fractionation as a function of (b) $[\text{CO}_{2,\text{aq}}]$, (c) μ_i , and (d) $\mu_i/[\text{CO}_{2,\text{aq}}]$ at a 16 h : 8 h (full symbols) or a 24 h : 0 h L/D cycle. The threshold concentration C_{lim} at or below which $[\text{CO}_{2,\text{aq}}]$ affects μ_i is indicated by the dashed line. Corresponding values of μ_i or ϵ_p are indicated by triangles.

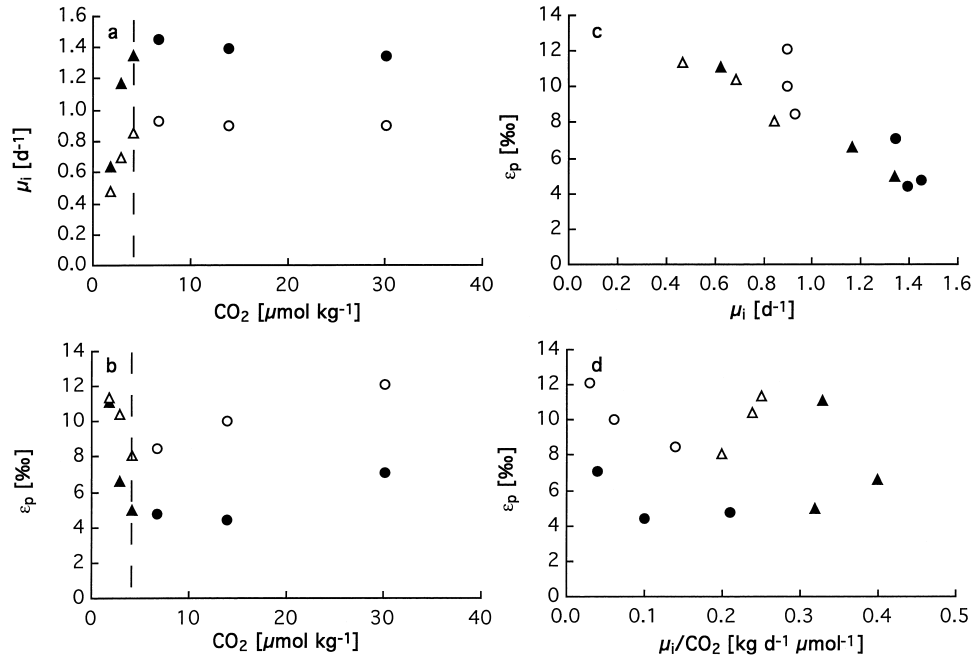


Fig. 3. *Thalassiosira punctigera*. (a) Instantaneous growth rate (μ_i) as a function of $[\text{CO}_{2,\text{aq}}]$, and stable carbon isotope fractionation as a function of (b) $[\text{CO}_{2,\text{aq}}]$, (c) μ_i , and (d) $\mu_i/[\text{CO}_{2,\text{aq}}]$ for two irradiance cycles. Symbols and indication of C_{lim} as in Figure 2.

punctigera (Fig. 3c) and *C. waielsii* (Fig. 4c) without much scatter caused by an additional CO_2 effect on ε_p . In *A. glacialis*, on the other hand, the effect on ε_p caused by changes in μ_i at

different irradiance cycles is masked by the effect of $[\text{CO}_{2,\text{aq}}]$ (Fig. 2c). No correlation between ε_p and μ_i was detected in *P. tricornutum* and in *S. trochoidea*. As indicated in Fig. 1c, ε_p

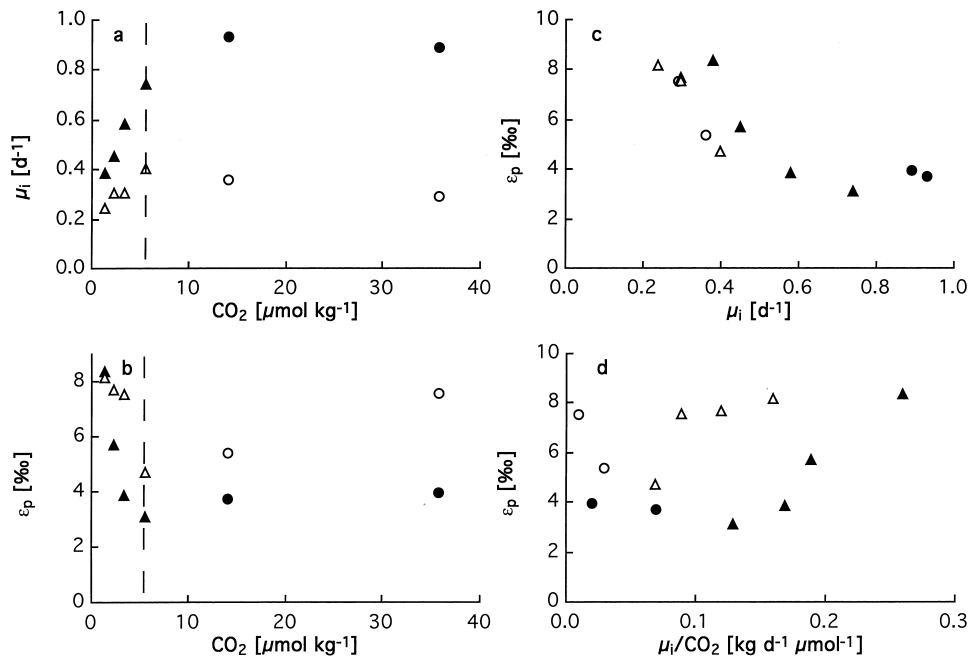


Fig. 4. *Coscinodiscus waielsii*. (a) Instantaneous growth rate (μ_i) as a function of $[\text{CO}_{2,\text{aq}}]$, and stable carbon isotope fractionation as a function of (b) $[\text{CO}_{2,\text{aq}}]$, (c) μ_i , and (d) $\mu_i/[\text{CO}_{2,\text{aq}}]$ for two irradiance cycles. Symbols and indication of C_{lim} as in Figure 2.

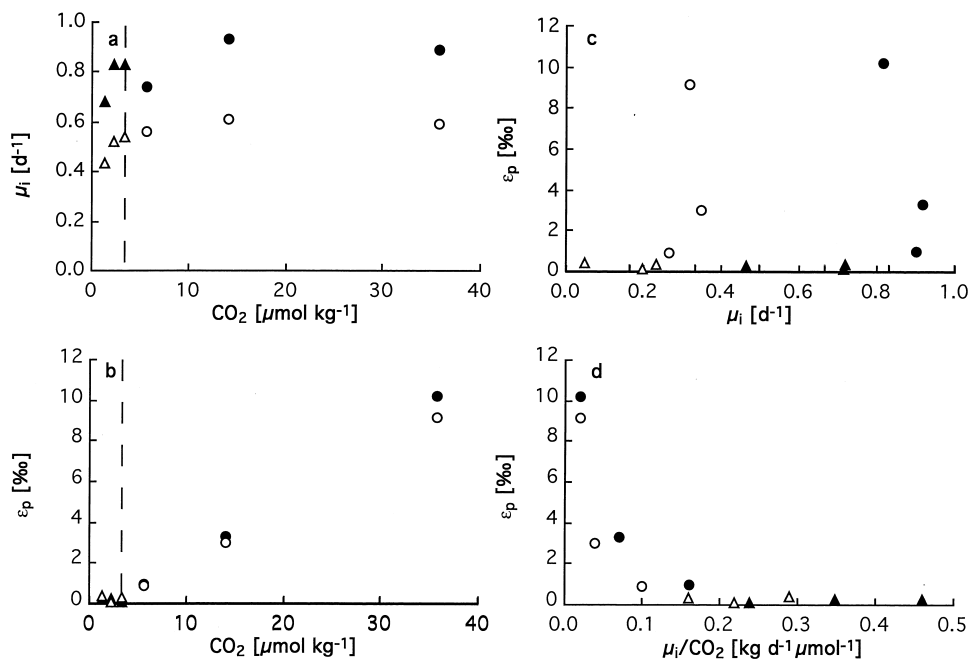


Fig. 5. *Scrippsiella trochoidea*. (a) Instantaneous growth rate (μ_i) as a function of $[\text{CO}_{2,\text{aq}}]$, and stable carbon isotope fractionation as a function of (b) $[\text{CO}_{2,\text{aq}}]$, (c) μ_i , and (d) $\mu_i/[\text{CO}_{2,\text{aq}}]$ for two irradiance cycles. Symbols and indication of C_{lim} as in Figure 2.

values of *P. tricorutum* range from ca. 10 to 16‰ in either irradiance cycle at a constant growth rate. Consequently, a relatively large residual variability ($r^2 = 0.714$) remains in the linear correlation between ε_p and $\mu_i/[\text{CO}_{2,\text{aq}}]$ in this diatom (Fig. 1d). A consistent but curvilinear decrease in ε_p with increasing $\mu_i/[\text{CO}_{2,\text{aq}}]$ was found in *A. glacialis* (Fig. 2d) and *S. trochoidea* (Fig. 5d). No significant trend for combined data of the two irradiance cycles were observed in *T. punctigera* (Fig. 3d) and *C. wailesii* (Fig. 4d), even when ε_p values from incubations below C_{lim} were excluded.

4. THEORETICAL BACKGROUND

4.1. Fractionation as a Function of C Fluxes

To provide the framework for our discussion of factors contributing to the observed variability in ε_p , we first introduce a simple conceptual fractionation model. In contrast to most existing models, it permits the simultaneous uptake of both CO_2 and HCO_3^- at variable proportions. Eqn. 5 describes isotopic fractionation as a function of the carbon fluxes associated with phytoplankton carbon acquisition, where ε_p is defined as

$$\varepsilon_p = a(\varepsilon_3 + \varepsilon_4) + (1 - a)\varepsilon_1 + (\varepsilon_2 - \varepsilon_{-1}) \frac{F_{-1}}{F_1 + F_4} \quad (5)$$

F_1 and F_{-1} are CO_2 fluxes into and out of the cell, respectively. F_4 is the flux of HCO_3^- into the cell, and a is the fractional contribution of HCO_3^- flux to gross total carbon uptake ($F_t = F_1 + F_4$) into the cell. Enzymatic fractionation during C fixation is denoted by ε_2 , equilibrium fractionation between CO_2 and HCO_3^- is denoted by ε_3 (please note that ε_3 assumes

negative values in this model). Fractionation associated with the influx and outflux of CO_2 (ε_1 , ε_{-1}) and with the uptake of HCO_3^- (ε_4) is often assumed to be on the order of ca. 1‰ (Raven, 1997; Keller and Morel, 1999), which is small compared with values up to 30‰ fractionation by the carbon-fixing enzyme RUBISCO (Roeske and O'Leary, 1984; Guy et al., 1993) and -10 ‰ for ε_3 under our experimental conditions. If we consider fractionation during inorganic carbon flux across the plasmalemma negligible, Eqn. 5 is approximated by

$$\varepsilon_p = a\varepsilon_3 + \varepsilon_2 \frac{F_{-1}}{F_t} \quad (6)$$

Diffusive loss of CO_2 from the cell back to the medium relative to gross total carbon uptake is termed "leakage" ($L = F_{-1}/F_t$). The model does not take HCO_3^- efflux into account, which has been suggested to constitute a significant portion of inorganic carbon loss in cyanobacteria (Salon et al., 1996). Based on mass balance considerations, C flux into organic carbon (F_2) during photosynthetic C fixation equals the difference between C uptake and C loss:

$$F_2 = F_t - F_{-1} \quad (7)$$

We can describe F_2 as the product of instantaneous growth rate (μ_i) and cellular carbon content (γ_C), which represents the carbon-specific growth rate μ_c :

$$\mu_c = \mu_i \gamma_C \quad (8)$$

By using Eqns. 6–8, we can now define isotopic fractionation as a function of growth rate:

Table 1. Cellular carbon content, γ_C , and cell surface area, S. Mean γ_C (± 1 SD) is shown for six CO_2 concentrations and two L/D cycles. Mean S (± 1 SD) is shown as combined data for the two L/D cycles.

Species	L/D cycle [h : h]	C/cell (γ_C) [pmol cell ⁻¹]	Cell surface area (S) [μm^2]
<i>P. tricornutum</i>	16 : 8	$7.4 (\pm 0.6) \times 10^{-1}$	$6.9 (\pm 0.2) \times 10^1$
	24 : 0	$7.6 (\pm 0.6) \times 10^{-1}$	
<i>A. glacialis</i>	16 : 8	$9.7 (\pm 0.6) \times 10^0$	$4.1 (\pm 0.3) \times 10^2$
	24 : 0	$7.9 (\pm 0.7) \times 10^0$	
<i>T. punctigera</i>	16 : 8	$1.8 (\pm 0.1) \times 10^2$	$5.8 (\pm 0.4) \times 10^3$
	24 : 0	$1.5 (\pm 0.1) \times 10^2$	
<i>C. walesii</i>	16 : 8	$3.6 (\pm 0.2) \times 10^4$	$1.1 (\pm 0.3) \times 10^5$
	24 : 0	$3.8 (\pm 0.3) \times 10^4$	
<i>S. trochoidea</i>	16 : 8	$5.9 (\pm 0.8) \times 10^1$	$3.3 (\pm 0.3) \times 10^3$
	24 : 0	$5.4 (\pm 0.4) \times 10^1$	

$$\varepsilon_p = a \varepsilon_3 + \varepsilon_2 - \varepsilon_2 \frac{\mu_c}{F_t} \quad (9)$$

This general formulation accounts for carbon uptake of CO_2 and/or HCO_3^- irrespective of the mechanism by which inorganic carbon passes the membrane. CO_2 may enter the cell by passive diffusion or active transport. Due to the low permeability of biological membranes for the charged molecule HCO_3^- , it is usually assumed that HCO_3^- can enter an algal cell only by an energy-dependent uptake mechanism (see Raven, 1997, for review) and that inorganic carbon leaves the cell only by passive diffusion of CO_2 . Further assumptions made in this model are that: (1) the cell consists of a single compartment; (2) fractionation associated with C loss due to respiration or photorespiration is negligible; and (3) all HCO_3^- entering the cell is converted into CO_2 before it becomes fixed into organic C compounds or is lost from the cell (i.e., no fractionation is associated with this reaction). If all inorganic carbon is taken up as CO_2 ($a = 0$, $F_t = F_1$) and fractionation associated with carbon flux across the plasmalemma is considered negligible (ε_1 , $\varepsilon_{-1} = 0$), the model is identical with the fractionation models suggested by Francois et al. (1993) and Laws et al. (1995). If all inorganic carbon is taken up by active transport of HCO_3^- ($a = 1$, $F_t = F_4$) and no fractionation occurs during C flux across the plasmalemma (ε_4 , $\varepsilon_{-1} = 0$), the model is identical with the carbon concentrating model suggested by Sharkey and Berry (1985).

Precise measurements of fractionation during C fixation (ε_2) are not available for eukaryotic microalgae. For the carbon-fixing enzyme RUBISCO, isolated from spinach, Roeske and O'Leary (1984) report ε_2 values of 30‰ (pH 7.0), 29‰ (pH 8.0), and 26‰ (pH 9.0), which is similar to $\varepsilon_2 = 30.3$ ‰ (pH 8.5) determined by Guy et al. (1993). Thus, the effect of pH on ε_2 is small and is probably negligible in vivo (Guy et al., 1993), if we consider maintenance of relatively constant pH levels inside the chloroplast, where RUBISCO is located.

In contrast to higher C_3 plants such as spinach, fractionation by RUBISCO is significantly lower in a photosynthetic bacterium and a cyanobacterium, with ε_2 values ranging between 17.8 and 23.0‰ depending on species and reaction conditions (Roeske and O'Leary, 1985; Guy et al., 1993). A comparison of kinetic and structural properties of RUBISCO (see Raven, 1997 and Badger et al., 1998, for recent reviews) suggests that ε_2 values of diatoms show greater similarity with higher C_3 plants

than with the low fractionation of photosynthetic bacteria. Direct evidence for high fractionation during carboxylation reactions in marine diatoms is given by direct measurements of $\varepsilon_p = 26$ ‰ in *P. tricornutum* (Laws et al., 1997; U.R., unpubl. data) at low $\mu/[\text{CO}_{2,\text{aq}}]$, which implies $\varepsilon_2 \geq 26$ ‰. For the interpretation of our results, we thus adopted a constant ε_2 value of 27‰. This represents the mid-point of the range for maximum fractionation by all cellular carboxylation reactions (25.4–28.3‰) suggested by Goericke et al. (1994), which also accounts for fractionation by β -carboxylation.

If we assume that ε_2 does not differ between species and treatments, isotopic fractionation is only a function of growth rate relative to gross total C uptake, and of the relative contribution of HCO_3^- to the flux of inorganic carbon into the cell (Eqn. 9), because ε_3 was constant in our experiments. Instantaneous growth rates of each species were approximately proportional to carbon-specific growth rates, as cellular carbon content exhibited no systematic trend over the experimental CO_2 range and differences in γ_C between irradiance cycles were small (Table 1).

4.2. Minimum $[\text{CO}_{2,\text{aq}}]$ for Diffusive C Uptake

The fractionation model provides a tool to estimate the minimum CO_2 concentration at which the uncatalyzed diffusive supply of carbon dioxide to the cell surface is sufficient to account for the observed rate of gross carbon uptake. Diffusive flux of CO_2 to an algal cell (F_r) can be calculated as

$$F_r = 4 \pi r D \left(1 + \frac{r_s}{r_k} \right) ([\text{CO}_{2,\text{aq}}] - C_r) \quad (10)$$

where r_s is the surface-equivalent spherical cell radius, D is the diffusion coefficient for CO_2 in the medium, r_k is the reacto-diffusive length, and C_r is the CO_2 concentration at the cell surface (Riebesell et al., 1993; Wolf-Gladrow and Riebesell, 1997). Maximum CO_2 flux to an algal cell can theoretically be achieved if C_r approaches 0 due to algal carbon uptake, corresponding to the maximum CO_2 gradient between the bulk medium and the cell surface. If we set $C_r = 0$ and maximum $F_r = F_1$, we can then calculate the minimum CO_2 concentration ($\text{CO}_{2,\text{min}}$) required to satisfy C flux into the cell by passive diffusion according to

$$\text{CO}_{2,\text{min}} = \frac{F_1}{4 \pi r D(1 + r/r_k)} \quad (11)$$

The value for F_1 is obtained from Eqn. 9 based on measurements of ε_p , μ_i , and cellular carbon content, assuming $\varepsilon_2 = 27\%$ and diffusive CO_2 uptake to be the only carbon source for photosynthesis (i.e., $a = 0$, $F_t = F_1$). The term $1 + r/r_k$ accounts for the contribution of extracellular uncatalyzed HCO_3^- - CO_2 conversion to total CO_2 supply and was calculated according to Wolf-Gladrow and Riebesell (1997). A CO_2 diffusion coefficient of $D = 1.45 \times 10^{-9} \text{ m}^2 \text{ s}^{-1}$ at 15°C (Rau et al., 1996) was used for all calculations of $\text{CO}_{2,\text{min}}$.

5. DISCUSSION

A central aspect for the interpretation of stable carbon isotope fractionation is the mechanism of inorganic carbon acquisition in marine phytoplankton. In the case that cellular carbon uptake is dominated by passive diffusion of CO_2 across the plasmalemma, any change in $[\text{CO}_{2,\text{aq}}]$ directly affects the flux of inorganic carbon into the cell. Below a critical CO_2 concentration, diminishing CO_2 supply leads to a decrease in growth rate. Under these conditions, a simple linear relationship between isotopic fractionation and $\mu/[\text{CO}_{2,\text{aq}}]$ is predicted from fractionation models (e.g., Francois et al., 1993; Goericke et al., 1994; Laws et al., 1995; Rau et al., 1996).

Catalyzed conversion of HCO_3^- to CO_2 by extracellular carbonic anhydrase (CA) may significantly accelerate the rate of CO_2 supply to the cell surface. Isotopic fractionation in this scenario may be indistinguishable from CO_2 uptake in the absence of CA (Riebesell and Wolf-Gladrow, 1995). However, the correlation between ε_p and bulk $[\text{CO}_{2,\text{aq}}]$ is less predictable if the CO_2 concentration near the cell surface is not only a function of $[\text{CO}_{2,\text{aq}}]$ but also of CA activity.

Active uptake of inorganic carbon adds further complexity to the interpretation of isotope data. Energy-dependent uptake of both CO_2 and/or HCO_3^- has been suggested in several microalgae (for recent reviews, see Raven, 1997; Kaplan and Reinhold, 1999). Compared to CO_2 uptake, the transport of HCO_3^- through the plasmalemma alters the isotopic composition of the inorganic carbon pool inside the cell, which translates into a change in ε_p . If HCO_3^- is taken up directly from the medium, growth rate becomes independent of extracellular CO_2 concentrations. Regardless of the carbon species entering the cell, regulated active C transport can affect the ratio of C uptake to growth rate, which is a critical parameter in isotopic fractionation.

In the following, we discuss our experimental results with respect to different carbon acquisition scenarios. We apply several criteria to evaluate the possibility of diffusive CO_2 uptake and consider the potential consequences of active carbon transport for the interpretation of isotope data.

5.1. Diffusive vs. Active Carbon Uptake

To distinguish between uncatalyzed diffusive CO_2 uptake and CA-mediated HCO_3^- utilization or active uptake of inorganic carbon in our experiments, we considered the following parameters: the critical CO_2 concentration (C_{min}) below which cellular C demand cannot be satisfied by passive diffusion alone, the daylength-related variability in ε_p at constant

$[\text{CO}_{2,\text{aq}}]$, and the linearity of the relationship between ε_p and $\mu_i/[\text{CO}_{2,\text{aq}}]$.

In most species and treatments, bulk concentrations of CO_2 were several-fold higher than the minimum CO_2 concentration required for diffusive CO_2 uptake (Fig. 6). These results indicate that most species were theoretically able to satisfy their cellular carbon demand at all experimental CO_2 levels by diffusive CO_2 uptake even in the absence of extracellular CA. In contrast to the smaller species, $\text{CO}_{2,\text{min}}$ of *C. walesii* was one order of magnitude higher and exceeded $[\text{CO}_{2,\text{aq}}]$ in all treatments. These cells require an additional carbon source, either by the CA-catalyzed conversion of HCO_3^- to CO_2 near the cell surface with subsequent CO_2 uptake, or by direct transport of HCO_3^- through the plasmalemma. Similarly, extracellular CA activity or direct HCO_3^- uptake is necessary to account for the carbon demand of *T. punctigera* at $[\text{CO}_{2,\text{aq}}] < 5 \mu\text{mol kg}^{-1}$ in this study.

According to the diffusion model, any change in growth rate at a given CO_2 concentration should be reflected in variable ε_p . In *P. tricorutum* and in *S. trochoidea*, isotopic fractionation was unaffected by daylength at each $[\text{CO}_{2,\text{aq}}]$ despite significant differences in μ_i . We take this as evidence for a regulated carbon acquisition mechanism in these species even at the highest experimental CO_2 concentration. In the other three species, daylength-related differences in ε_p are consistent with uncatalyzed diffusive CO_2 uptake, but do not exclude the possibility of extracellular CA activity or active carbon transport.

Another prediction by the diffusion model is a linear, inverse relationship between ε_p and $\mu_i/[\text{CO}_{2,\text{aq}}]$ with ε_p close to enzymatic fractionation as $\mu_i/[\text{CO}_{2,\text{aq}}]$ approaches 0. In four of the species tested, the lack of such a linear correlation suggests that mechanisms other than uncatalyzed passive diffusion are involved in carbon acquisition of these species. The relatively large scatter in the ε_p vs. $\mu_i/[\text{CO}_{2,\text{aq}}]$ relationship of *P. tricorutum* may also result from regulated C uptake. Furthermore, the y-intercept of the corresponding regression line in this species is approximately 17‰, which is far below the expected value of 25–28‰ (Raven and Johnston, 1991; Goericke et al., 1994) in the case of diffusive CO_2 uptake.

5.2. CO_2 vs. HCO_3^- Uptake

We applied three criteria to extract information from our experimental data regarding the carbon species entering the cell: CO_2 -related variability in ε_p at a constant growth rate, simultaneous changes in ε_p and growth rate at variable $[\text{CO}_{2,\text{aq}}]$, and maximum fractionation achieved at the highest CO_2 concentration.

In all species tested, growth rate was largely independent of $[\text{CO}_{2,\text{aq}}]$ over a wide range of CO_2 concentrations, whereas ε_p decreased towards lower $[\text{CO}_{2,\text{aq}}]$ in this range. It is unlikely that direct uptake of HCO_3^- as the only carbon source can account for the observed pattern, because fractionation is expected to remain constant in that case. Two different scenarios, however, could explain the data.

In the first scenario, CO_2 is the dominant carbon species entering the cell, either by passive diffusion (possibly in combination with extracellular CA activity) or by active transport of CO_2 . If a decrease in $[\text{CO}_{2,\text{aq}}]$ results in diminishing CO_2

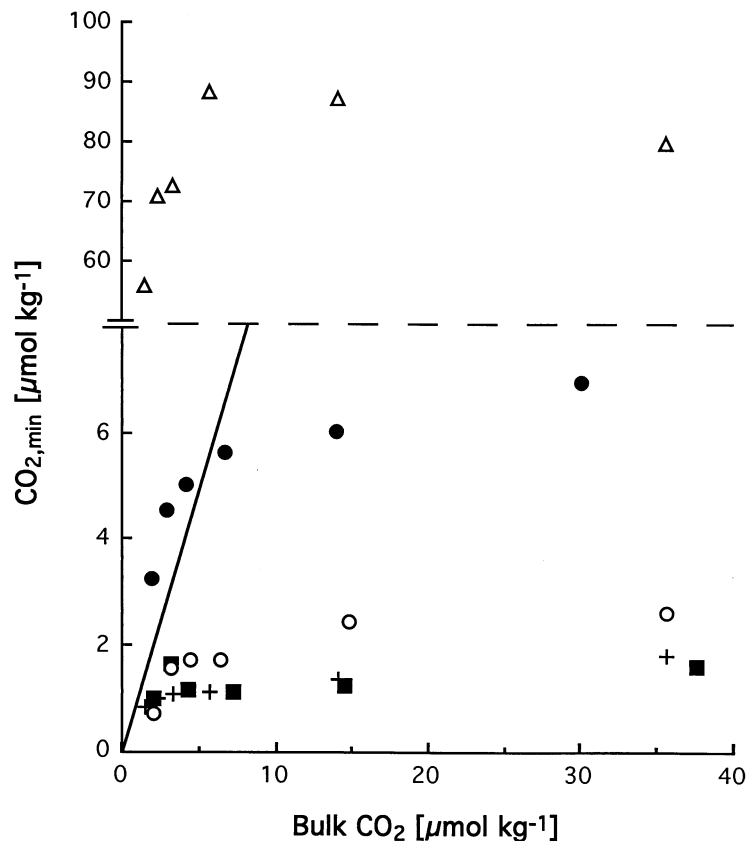


Fig. 6. Minimum CO_2 concentration (C_{\min}) required for diffusive CO_2 uptake as a function of bulk $[\text{CO}_{2,\text{aq}}]$. C_{\min} was calculated for *P. tricornutum* (■), *A. glacialis* (○), *T. punctigera* (●), *C. wailesii* (△), and *S. trochoidea* (+) during growth under continuous light. The reference line indicates $C_{\min} = [\text{CO}_{2,\text{aq}}]$. Above this line, uncatalyzed diffusive CO_2 supply is insufficient to account for algal C uptake. Please note differences in scale on the y-axis. C_{\min} in *C. wailesii* is approximately one order of magnitude higher than in the smaller species.

uptake rates (F_1), ε_p decreases due to an increase in the ratio μ_i/F_1 as long as the carbon supply is high enough to maintain a constant growth rate. An algal cell may possess several options to achieve such an increase in C assimilation efficiency (i.e., reduce leakage of CO_2), as will be discussed below.

Alternatively, the decrease in ε_p toward lower CO_2 concentrations may result from the gradual induction of HCO_3^- transport across the plasmalemma in addition to CO_2 uptake. In this scenario, the cell is able to maintain a constant rate of gross C uptake. The apparent shift in ε_p results from the higher fractional contribution of HCO_3^- to total C flux into the cell at lower $[\text{CO}_{2,\text{aq}}]$.

Regardless of the differences between the two scenarios, a significant contribution of CO_2 to total carbon uptake is a prerequisite in both cases to account for the CO_2 -related changes in ε_p at a constant growth rate in this study.

With the exception of *P. tricornutum*, growth rate declined in all species below a critical CO_2 concentration (C_{lim}). In this CO_2 range, isotopic fractionation did not further decrease but even increased upon a decline in $[\text{CO}_{2,\text{aq}}]$. If the cells can take up HCO_3^- directly from the medium, neither a CO_2 -related decline in growth rate nor a corresponding increase in ε_p would be expected. On the other hand, the observed pattern is consistent with CO_2 transport into the cell: at $[\text{CO}_{2,\text{aq}}] < C_{\text{lim}}$, any

increase in ε_p towards lower CO_2 concentrations requires that a decrease in the carbon uptake rate is accompanied by an even larger decline in growth rate. Calculations according to Eqn. 9 (assuming $a = 0$, $\varepsilon_2 = 27\text{‰}$) indicate that the measured decrease in μ_i by 53% (*T. punctigera*) and 49% (*C. wailesii*) leads to the observed increase in ε_p if F_1 declines by 35% or 34%, respectively.

Such a decline in C assimilation efficiency (i.e., a decrease in μ_i/F_1) towards lower $[\text{CO}_{2,\text{aq}}]$ is expected for several reasons. First, the probability of diffusive CO_2 loss from the cell back into the medium increases with diminishing $[\text{CO}_{2,\text{aq}}]$, so that a smaller fraction of gross total carbon uptake is available for cellular growth. Second, it is reasonable to assume that the carbon-fixing enzyme RUBISCO shows nonlinear saturation kinetics. Therefore, a decline in substrate (i.e., CO_2) concentration in response to diminishing carbon uptake rates is likely to result in an unproportionally stronger decline in the rate of CO_2 fixation. Third, in the case of active CO_2 uptake, the ratio of C uptake to C fixation can be affected by the availability of energy (ATP) and reducing power (NADPH_2) at low $[\text{CO}_{2,\text{aq}}]$. Under high-light and nutrient-replete conditions, yet at low $[\text{CO}_{2,\text{aq}}]$, substrate limitation of CO_2 fixation in the Calvin cycle decreases the demand for both ATP and NADPH_2 , which results in the accumulation of electrons in the light-dependent

photosynthesis reactions. Pseudocyclic electron flow (Mehler reaction), which ultimately leads to the reduction of oxygen within the cell, may serve as an electron sink to dissipate excess light energy (Sültemeyer et al., 1993; Kaplan and Reinhold, 1999). Because the Mehler reaction generates additional ATP (but not NADPH₂), active CO₂ transport (which requires energy but not reducing power) may be less affected by diminishing CO₂ supply than by the rate of carbon fixation.

Another potential tool to distinguish between CO₂ and HCO₃⁻ uptake is the maximum fractionation achieved by a cell. Isotopic fractionation cannot exceed maximum fractionation in carboxylation reactions, which has been suggested to lie in the range of 25.4–28.3‰ (Goerick et al., 1994). Direct measurements of ϵ_p in *P. tricornutum* revealed values up to 25.72‰ (Laws et al., 1997) at [CO_{2, aq}] = 34.7 μmol kg⁻¹ and $\mu_i = 0.5$ d⁻¹. Such high ϵ_p values cannot be obtained by HCO₃⁻ uptake. In fact, even in the case of exclusive CO₂ uptake, approximately 90% leakage (diffusive loss of CO₂ back to the medium) is required to account for the observed fractionation when $\epsilon_2 = 28.3$ ‰ is assumed (Eqn. 6).

At a similar CO₂ concentration in our study, ϵ_p was approximately 10‰ lower. A comparison with the ϵ_p vs. μ_i /[CO_{2, aq}] relationship of Laws et al. (1995) indicates that the higher growth rate in our experiments (L/D 24:0, $\mu_i = 1.63$ d⁻¹, [CO_{2, aq}] = 37.7 μmol kg⁻¹) would account for approximately half of the difference in ϵ_p between the two studies. Alternatively, differences in the kind of growth limitation may account for much of the observed difference in ϵ_p . A potential effect of N limitation on isotopic fractionation has been suggested by Kukert and Riebesell (1998) for field data and by Riebesell et al. (submitted). In the latter study, fractionation of *P. tricornutum* at different light intensities and [CO_{2, aq}] was compared with results for this species reported by Johnston (1996), Laws et al. (1997), and in this article. A comparison of recent data by Riebesell (unpublished) with those of Bidigare et al. (1997), using the same strain of the coccolithophorid *E. huxleyi*, is consistent with the suggestion that N limitation yields higher ϵ_p at similar growth rates and [CO_{2, aq}].

Although isotopic fractionation of *P. tricornutum* in this study did not exceed 16.7‰, this value still provides evidence that HCO₃⁻ uptake did not dominate inorganic carbon flux into the cell. According to Eqns. 6 and 9, 90% leakage is required to achieve 16.7‰ fractionation in the case of HCO₃⁻ uptake. This is highly unlikely from an energetic point of view, because metabolic energy is spent for each HCO₃⁻ molecule entering the cell. Calculated leakage values are lower by approximately 40% in case that CO₂ is the only carbon species passing the plasmalemma. It should be pointed out that these calculations are based on the assumption that inorganic carbon loss from the cell occurs only as CO₂. Different results would be obtained if significant amounts of HCO₃⁻ can leave the cell, possibly by HCO₃⁻ : HCO₃⁻ exchange.

In all species, maximum fractionation was ca. 8 to 17‰, i.e., significantly lower than fractionation during carboxylation reactions. Higher values are expected upon a further increase in CO₂ concentration beyond the experimental range of our study. Due to the lack of a linear relationship between ϵ_p and μ_i /[CO_{2, aq}], this kind of analysis cannot be used to infer maximum ϵ_p values for the respective species from our data.

Nonlinear fits should be treated with caution until a mechanistic explanation for the variability in ϵ_p is established.

At this point in our discussion, we may conclude that CO₂ flux into the cell appears to constitute a significant portion of gross total carbon uptake in all species tested. Several lines of evidence, however, indicate that either active C transport and/or the activity of extracellular CA are required to account for the observed correlation of ϵ_p with [CO_{2, aq}] and growth rate. With the exception of *P. tricornutum*, a critical CO₂ concentration has been observed in all species, below which the cells are not able to maintain a constant growth rate. Even if these organisms possess a mechanism for direct uptake of HCO₃⁻, it is insufficient to compensate for the diminishing CO₂ supply. In experiments with *P. tricornutum*, the lowest experimental [CO_{2, aq}] was 2.1 μmol kg⁻¹. It could be that the critical CO₂ level for C-limited growth is reached at an even lower CO₂ concentration due to the small cell size of this species. This could be tested in further experiments at [CO_{2, aq}] < 2 μmol kg⁻¹. Alternatively, it is possible that *P. tricornutum* differs from the other species in our study in its ability to rely on HCO₃⁻ uptake at low [CO_{2, aq}], so that growth rate becomes independent of CO₂ supply at any CO₂ concentration. The presence of a facultative uptake system for HCO₃⁻ in *P. tricornutum* in the absence of extracellular CA has been demonstrated in previous studies (Rotatore et al., 1995; Colman and Rotatore, 1995).

5.3. Taxonomic Differences in Fractionation

Although the correlation of ϵ_p with [CO_{2, aq}] and μ_i shows the same general trends in *S. trochoidea* as in the diatoms, fractionation by the dinoflagellate appears to differ in some aspects from that of the other species. Fractionation is lower than in *T. punctigera*, with ϵ_p values close to 0 in some treatments, although higher values would be expected due to smaller cell size and lower growth rates. Fractionation by the dinoflagellate is more sensitive to changes in experimental [CO_{2, aq}] than fractionation by any of the diatom species in our study.

Taxonomic differences between diatoms and dinoflagellates with respect to both cell morphology and physiology may account for the observed differences in ϵ_p responses. Whereas chloroplasts and other cell organelles of diatoms are usually located in a relatively thin peripheral layer of cytoplasm between the cell wall and one or two large central vacuoles (Round et al., 1990), dinoflagellates lack such vacuoles and cell organelles are distributed over the entire cell (Van den Hoek, 1995). Another difference between the taxa is the presence of a membrane surrounding the cellulose cell wall of thecate dinoflagellates. Diatoms, in contrast, lack such a membrane around their silicate cell wall (Van den Hoek, 1995). Both the presence of an outer membrane and the distribution of chloroplasts throughout the cell may provide additional diffusive resistance for CO₂ to reach the site of carboxylation, which could contribute to the greater sensitivity of ϵ_p to variation in [CO_{2, aq}] in *S. trochoidea*.

Compared to diatoms, dinoflagellates have higher rates of dark respiration relative to growth rate (Geider and Osborne, 1989) so that our calculations of μ_i for *S. trochoidea* may underestimate the actual rate of instantaneous growth. Higher

μ_i would lead to lower ε_p values than in diatoms under otherwise similar conditions, which is consistent with our observations. Furthermore, β -carboxylation in dinoflagellates may differ from diatoms in both the carboxylating enzyme [e.g., pyruvate carboxylase (PC) in *S. trochoidea*; PEP carboxykinase (PEPCK) in *P. tricornutum* and *A. glacialis*] and the ratio of β -carboxylase to RUBISCO activity [e.g., 0.55 in *S. trochoidea*, but 0.03 in *P. tricornutum* and 0.11 in *A. glacialis*] (Descolas-Gros and Oriol, 1992). Whether differences in β -carboxylation activity are reflected in ε_p , however, depends on the ultimate fate of CO_2 involved in these reactions (no effect on ε_p if CO_2 is released again shortly after fixation; Raven, 1997) and on fractionation by the carboxylating enzyme. Although fractionation by PEPCK shows considerable overlap with RUBISCO (Arnelle and O'Leary, 1992), fractionation by PC has not been directly measured yet.

Finally, recent studies report the presence of form II RUBISCO in several dinoflagellate species (Morse et al., 1995; Whitney and Yellowlees, 1995). The structural similarity to RUBISCO of photosynthetic bacteria indicates that ε_p in dinoflagellates may also be significantly lower than in diatoms such as *P. tricornutum*, which possess form I RUBISCO. Again, lower ε_p values would be expected, which is consistent with our experiments with the dinoflagellate *S. trochoidea*.

5.4. Effect of Cell Size on the Relationship of ε_p with $\mu_i/[\text{CO}_{2,\text{aq}}]$

If we consider the entire experimental CO_2 range in our study, we find significant deviations from a linear relationship between ε_p and $\mu_i/[\text{CO}_{2,\text{aq}}]$ in all species tested, which we attribute to carbon acquisition by processes other than passive diffusion of CO_2 . This observation is consistent with the results of Laws et al. (1997) for *P. tricornutum*. In contemporary ocean surface waters, however, CO_2 concentrations below 7 to 10 $\mu\text{mol kg}^{-1}$ are rarely found. To test the applicability of a linear ε_p vs $\mu_i/[\text{CO}_{2,\text{aq}}]$ relationship at CO_2 concentrations typically encountered by phytoplankton under natural conditions, we selected data that were obtained from incubation at $[\text{CO}_{2,\text{aq}}] > 10 \mu\text{mol kg}^{-1}$ (Fig. 7). In addition to results from this study, we included values for the diatoms *S. costatum* (Burkhardt et al., 1999), *P. tricornutum* (Laws et al., 1995, 1997), and *P. glacialis* (Popp et al., 1998). The large scatter in Fig. 7a indicates that factors other than μ_i and $[\text{CO}_{2,\text{aq}}]$ need to be considered to explain the variability in ε_p .

An important aspect that has not yet been accounted for in our discussion is the large variation in cell size and cellular carbon content. In our experiments, variation in cellular carbon content (γ_C , [$\mu\text{mol C cell}^{-1}$]) for any given species was small (Table 1). Therefore, instantaneous growth rate μ_i , which does not account for differences in cellular carbon content, was sufficient in our analysis of isotopic fractionation. On the other hand, carbon-specific growth rate μ_c , defined as the product of γ_C and μ_i (Eqn. 8) is more appropriate to describe ε_p when comparing cells of different size. Several authors recognized the potential effect of cell size on isotopic fractionation (e.g., Laws et al., 1995; Rau et al., 1996) which has also been demonstrated based on experimental data (Popp et al., 1998). Because carbon flux through the plasmalemma should be roughly proportional to the cell surface area, Popp et al. (1998)

suggested that differences in the surface area and in the cellular C content between species may account for the differences in ε_p vs $\mu_i/[\text{CO}_{2,\text{aq}}]$ regressions. To test this, we plotted fractionation data from Figure 7a as a function of $\mu_c/(S [\text{CO}_{2,\text{aq}}])$ (Fig. 7b). Whereas cellular carbon content was directly estimated from mass spectrometric POC measurements and cell counts, cell surface area (S , [μm^2]; Table 1) was determined microscopically by taking differences in cell geometry into account.

Our results indicate that the scatter observed in Figure 7a is reduced by considering cellular carbon content and surface area (Fig. 7b). Similar results were obtained when we used cell volume (V) rather than carbon content in combination with surface area to correct for differences in cell size (data not shown). In contrast to the linear regression shown by Popp et al. (1998), a curvilinear relationship seems more appropriate to describe the relationship between ε_p and $\mu_c/(S [\text{CO}_{2,\text{aq}}])$ or $\mu_i V/(S [\text{CO}_{2,\text{aq}}])$, even when CO_2 concentrations below 10 $\mu\text{mol kg}^{-1}$ were excluded from the analysis. The flattening slope at $\mu_c/(S [\text{CO}_{2,\text{aq}}]) > 0.002$ (Fig. 7b) can be attributed largely to the unusually high cellular carbon content of *C. wailesii*, whereas μ_i of this species (0.24–0.93 d^{-1}) lies within the range of growth rates frequently encountered in the field.

Although both a linear and a curvilinear relationship may yield similar results at $\mu_c/(S [\text{CO}_{2,\text{aq}}]) < 0.002$, a general applicability of either function is still questionable because of the large residual variability in ε_p for any given value on the x-axis. For a given value of $\mu_c/(S [\text{CO}_{2,\text{aq}}]) = 6 (\pm 1) \times 10^4$, isotopic fractionation varies between 3.0 and 20.6‰. Lowest ε_p values are found in the dinoflagellate *S. trochoidea* (3.0‰) and in the antarctic diatom *P. glacialis* (6.0‰), intermediate values for small diatoms grown under nutrient-replete conditions (*S. costatum*: 13.8–14.4‰; *P. tricornutum*: 15.6‰), and maximum values for *P. tricornutum* (20.6‰) grown under nitrogen limitation. Factors that may be responsible for this residual variability include taxon-, species-, and strain-specific differences in the mechanism of inorganic carbon acquisition. Regulated active carbon transport, induction of HCO_3^- uptake, presence of extracellular CA, and differences in fractionation and kinetic properties of RUBISCO may lead to significant deviations of ε_p from model predictions. The particulate case of dinoflagellates has been discussed in the previous section. A comparison of field data by Kukert and Riebesell (1998) also indicates a large scatter in the ε_p vs. $\mu_i/[\text{CO}_{2,\text{aq}}]$ relationship. The authors suggested that, aside from variation in cell size, cellular C content, and taxon-specific differences, the nutritional status of the phytoplankton may determine ε_p . This is consistent with the observation by Riebesell et al. (submitted), who reported that isotopic fractionation is also determined by the factor controlling growth rate.

Popp et al. (1998) demonstrated that the applicability of the relationship between ε_p and $\mu_c/(S [\text{CO}_{2,\text{aq}}])$ to field data depends, at least, on a knowledge of μ_i and cell size (from which cellular C content may be estimated), which complicates or even prevents the use of isotope data for the reconstruction of paleo- $[\text{CO}_{2,\text{aq}}]$ from mixed plankton samples. Our experimental results add further complexity to the dependence of isotopic fractionation on environmental and species-specific factors, indicating that no general relationship between ε_p , $[\text{CO}_{2,\text{aq}}]$, and growth rate may exist which can be applied after correction for cellular C content and cell geometry.

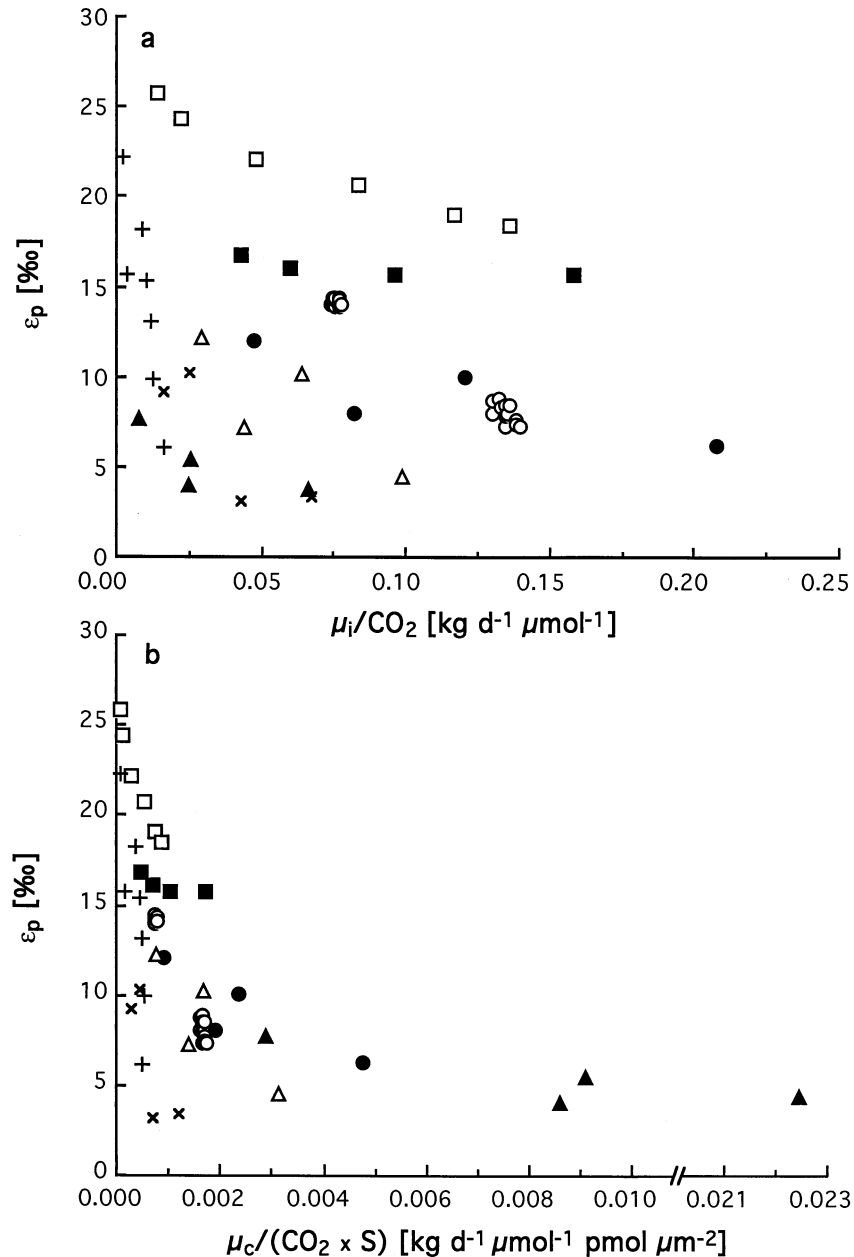


Fig. 7. Correlation of ϵ_p with (a) $\mu_i/[\text{CO}_{2,\text{aq}}]$ and (b) $\mu_c/(\text{CO}_2 \times S)$ in marine phytoplankton grown at $[\text{CO}_{2,\text{aq}}] > 10 \mu\text{mol kg}^{-1}$. Data for *P. tricornutum* (■), *A. glacialis* (●), *T. punctigera* (△), *C. walesii* (▲), and *S. trochoidea* (×) are from this study. In addition, we included data for *P. tricornutum* (□; Laws et al., 1995), *P. glacialis* (+; Popp et al., 1998), and *S. costatum* (○; Burkhardt et al., 1999).

It has often been suggested that the use of species-specific or group-specific biomarkers in isotope studies of field data (e.g., Bidigare et al., 1997) may be a valuable alternative to the analysis of mixed plankton samples. In this case, taxon-specific differences can be ignored and size effects may be negligible. Still, if an independent parameter can be found to estimate growth rates in the past, the use of ϵ_p vs $\mu_i/[\text{CO}_{2,\text{aq}}]$ linear regressions for paleobarometry requires a careful investigation whether different kinds of growth limitation (e.g., by nutrients, light intensity, or daylength) affect the predicted relationship.

6. CONCLUSIONS

Our results clearly demonstrate that changes in CO_2 concentration affect isotopic fractionation independent of growth rate in all species tested. Under conditions at which $[\text{CO}_{2,\text{aq}}]$ had no significant effect on growth rate, we observed CO_2 -related variation in ϵ_p up to 10‰ depending on the species tested. With the exception of *P. tricornutum*, isotopic fractionation of all species was sensitive to changes in CO_2 at concentrations $> 10 \mu\text{mol kg}^{-1}$, which covers the range of $[\text{CO}_{2,\text{aq}}]$ typically found

in ocean surface waters. The observed correlation of ϵ_p with $[\text{CO}_{2,\text{aq}}]$ may be caused either by changes in the rate of CO_2 uptake, or by the gradual induction of HCO_3^- uptake upon a decline in CO_2 supply.

We conclude from our results that processes other than the uncatalyzed passive diffusion of CO_2 participate in photosynthetic carbon acquisition of all marine phytoplankton species tested. Several lines of evidence indicate that carbon transport through the plasmalemma and/or the chloroplast envelope is regulated even at the highest experimental $[\text{CO}_{2,\text{aq}}]$ and that CO_2 uptake represents a significant fraction of gross total C uptake. However, no decision can be made with respect to the carbon acquisition mechanisms based on isotope data alone, which is in accordance with comments by other authors (e.g., Laws et al., 1997; Popp et al., 1998; Keller and Morel, 1999).

Growth rate, cell size, and taxon affected isotopic fractionation in our study to a similar or even greater degree than CO_2 concentration. The effect of daylength and concomitant variability in the instantaneous growth rate on ϵ_p was species-specific. Limitation of growth rate by CO_2 supply below a critical $[\text{CO}_{2,\text{aq}}]$ resulted in an increase in ϵ_p upon a further decline in $[\text{CO}_{2,\text{aq}}]$. Differences in cell size between species affected both the absolute value of ϵ_p (at similar $[\text{CO}_{2,\text{aq}}]$ and growth rate) and the magnitude of CO_2 -related changes in ϵ_p . Furthermore, our data provide evidence for taxonomic differences in isotopic fractionation between the four diatoms and the dinoflagellate tested.

In contrast to Popp et al. (1998), who reported a systematic relationship between ϵ_p and $\mu/[\text{CO}_{2,\text{aq}}]$ (with different slopes but identical y-intercepts) in three eukaryotic microalgae, we observed significant deviations from this correlation in the five species of marine phytoplankton tested here, even when accounting for differences in cellular carbon content and cell geometry. Both differences in growth conditions between these studies and differences in species-specific carbon acquisition mechanisms may account for the variability in size-corrected ϵ_p vs. $\mu/[\text{CO}_{2,\text{aq}}]$ regressions. The lack of a general relationship between ϵ_p and $\mu/[\text{CO}_{2,\text{aq}}]$ prevents the use of stable carbon isotopes, measured on POC of mixed phytoplankton assemblages, for the reconstruction of CO_2 even if parameters such as growth rate, cellular carbon content, and cell geometry are well constrained. This stresses the need to explore other possible relationships to adequately explain the observed ϵ_p - CO_2 dependence. Stable carbon isotopes in species-specific or taxon-specific compounds could provide a valuable option for the reconstruction of $[\text{CO}_{2,\text{aq}}]$. Their application, however, requires careful evaluation of the potential effects of irradiance cycles, light intensity, and nutrient limitation on isotopic fractionation in "biomarker species" before a reliable calibration for the correlation of ϵ_p with $[\text{CO}_{2,\text{aq}}]$ can be established.

Acknowledgments—We thank A. Dauelsberg, C. Hartmann, C. Langreder, A. Mackensen, K.-U. Richter, and G. Traue for technical support. This research was partly supported by the project Marine Ecosystem Regulation: Trace Metal and Carbon Dioxide Limitation (MERLIM) of the European Union within the Marine Science and Technology Program under Contract MAS3-CT95-0005. This is publication 1621 of the Alfred Wegener Institute for Polar and Marine Research.

REFERENCES

- Arnelo D. R. and O'Leary M. H. (1992) Binding of carbon dioxide on phosphoenol-pyruvate carboxykinase deduced from carbon kinetics isotope effects. *Biochemistry* **31**, 4363–4368.
- Badger M. R., Andrews T. J., Whitney S. M., Ludwig M., Yellowlees D. C., Leggat W., and Price G. D. (1998) The diversity and coevolution of Rubisco, plastids, pyrenoids and chloroplast-based CO_2 concentrating mechanisms in algae. *Can. J. Bot.* **76**, 1052–1071.
- Bigdare R. R., Fluegge A., Freeman K. H., Hanson K. L., Hayes J. M., Hollander D., Jasper J. P., King L. L., Laws E. A., Milder J., Millero F. J., Pancost R., Popp B. N., Steinberg P. A., and Wakeham S. G. (1997) Consistent fractionation of ^{13}C in nature and in the laboratory: Growth rate effects in some haptophyte algae. *Global Biogeochem. Cycles* **11**, 279–292.
- Burkhardt S., Riebesell U., and Zondervan I. (1999) Stable carbon isotope fractionation by marine phytoplankton in response to daylength, growth rate, and CO_2 availability. *Mar. Ecol. Prog. Ser.* **184**, 31–41.
- Colman B. and Rotatore C. (1995) Photosynthetic inorganic carbon uptake and accumulation in two marine diatoms. *Plant Cell Environ.* **18**, 919–924.
- Descolas-Gros C. and Oriol L. (1992) Variations in carboxylase activity in marine phytoplankton cultures. β -carboxylation in carbon flux studies. *Mar. Ecol. Prog. Ser.* **85**, 163–169.
- Francois R., Altabet M. A., and Goericke R. (1993) Changes in the $\delta^{13}\text{C}$ of surface water particulate organic matter across the subtropical convergence in the SW Indian Ocean. *Global Biogeochem. Cycles* **7**, 627–644.
- Freeman K. H. and Hayes J. M. (1992) Fractionation of carbon isotopes by phytoplankton and estimates of ancient CO_2 levels. *Global Biogeochem. Cycles* **6**, 185–198.
- Geider R. J. and Osborne B. A. (1989) Respiration and microalgal growth: A review of the quantitative relationship between dark respiration and growth. *New Phytol.* **112**, 327–341.
- Goericke R., Montoya J. P., and Fry B. (1994) Physiology of isotopic fractionation in algae and cyanobacteria. In *Stable Isotopes in Ecology and Environmental Science* (ed. K. Lajtha and R. H. Michener), pp. 187–221. Blackwell Science Publishers.
- Guillard R. R. L. and Ryther J. H. (1962) Studies of marine planktonic diatoms. *Can. J. Microbiol.* **8**, 229–239.
- Guy R. D., Fogel M. L., and Bery J. A. (1993) Photosynthetic fractionation of the stable isotopes of oxygen and carbon. *Plant Physiol.* **101**, 37–47.
- Jasper J. P., Hayes J. M., Mix A. C., and Prahl F. G. (1994) Photosynthetic fractionation of ^{13}C and concentrations of dissolved CO_2 in the central equatorial Pacific during the last 255,000 years. *Paleoceanography* **9**, 781–798.
- Johnston A. M. (1996) The effect of environmental variables on ^{13}C discrimination by two marine phytoplankton. *Mar. Ecol. Prog. Ser.* **132**, 257–263.
- Kaplan A. and Reinhold L. (1999) CO_2 concentrating mechanisms in photosynthetic microorganisms. *Ann. Rev. Plant Physiol. Plant Mol. Biol.* **50**, 539–570.
- Keller K. and Morel F. M. M. A model of carbon isotope discrimination and active carbon uptake in phytoplankton. *Mar. Ecol. Prog. Ser.* **182**, 295–298.
- Kukert H. and Riebesell U. (1998) Phytoplankton carbon isotope fractionation during a diatom spring bloom in a Norwegian fjord. *Mar. Ecol. Prog. Ser.* **173**, 127–137.
- Laws E. A. and Bannister T. T. (1980) Nutrient- and light-limited growth of *Thalassiosira fluviatilis* in continuous culture, with implications for phytoplankton growth in the ocean. *Limnol. Oceanogr.* **25**, 457–473.
- Laws E. A., Popp B. N., and Bigdare R. R. (1997) Effect of growth rate and CO_2 concentration on carbon isotopic fractionation by the marine diatom *Phaeodactylum tricorutum*. *Limnol. Oceanogr.* **42**, 1552–1560.
- Laws E. A., Popp B. N., Bigdare R. R., Kennicutt M. C., II, and Macko S. A. (1995) Dependence of phytoplankton carbon isotopic composition on growth rate and $[\text{CO}_2]_{\text{aq}}$: Theoretical considerations and experimental results. *Geochim. Cosmochim. Acta* **59**, 1131–1138.
- Mehrbach C., Culbertson C. H., Hawley J. E., and Pytkowicz R. M.

- (1973) Measurement of the apparent dissociation constants of carbonic acid in seawater at atmospheric pressure. *Limnol. Oceanogr.* **18**, 897–907.
- Mook W. G., Bommerson J. C., and Staverman W. H. (1974) Carbon isotope fractionation between dissolved bicarbonate and gaseous carbon dioxide. *Earth Planet. Sci. Lett.* **22**, 169–176.
- Morse D., Salois P., Markovic P., and Hastings J. W. (1995) A nuclear-encoded form II RuBisCO in dinoflagellates. *Science* **268**, 1622–1624.
- O'Leary M. H., Madhavan S., and Paneth P. (1992) Physical and chemical basis of carbon isotope fractionation in plants. *Plant Cell Environ.* **15**, 1099–1104.
- Popb B. N., Laws E. A., Bidigare R. R., Dore J. E., Hanson K. L., and Wakeham S. G. (1998) Effect of phytoplankton cell geometry on carbon isotopic fractionation. *Geochim. Cosmochim. Acta* **62**, 69–77.
- Rau G. (1994) Variations in sedimentary organic $\delta^{13}\text{C}$ as a proxy for past changes in ocean and atmospheric CO_2 concentrations. In *Carbon Cycling in the Glacial Ocean: Constraints on the Ocean's Role in Global Change* (eds. R. Zahn et al.), Vol. 17, pp. 307–321. NATO ASI Series 1.
- Rau G. H., Riebesell U., and Wolf-Gladrow D. (1996) A model of photosynthetic ^{13}C fractionation by marine phytoplankton based on diffusive molecular CO_2 uptake. *Mar. Ecol. Prog. Ser.* **133**, 275–285.
- Rau G., Sweeney R. E., and Kaplan I. R. (1982) Plankton $^{13}\text{C}/^{12}\text{C}$ ratio changes with latitude: Differences between northern and southern oceans. *Deep-Sea Res.* **29**, 1035–1039.
- Rau G., Takahashi T., and des Marais D. J. (1989) Latitudinal variations in plankton $\delta^{13}\text{C}$: Implications for CO_2 and productivity in past oceans. *Nature* **341**, 516–518.
- Rau G. H., Takahashi T., des Marais D. J., Repeta D. J., and Martin J. H. (1992) The relationship between $\delta^{13}\text{C}$ of organic matter and $[\text{CO}_2(\text{aq})]$ in ocean surface water: Data from a JGOFS site in the northeast Atlantic Ocean and a model. *Geochim. Cosmochim. Acta* **56**, 1413–1419.
- Raven J. A. (1997) Inorganic carbon acquisition by marine autotrophs. *Adv. Bot. Res.* **27**, 85–209.
- Raven J. A. and Johnston A. M. (1991) Inorganic carbon acquisition mechanisms in marine phytoplankton and their implications for the use of other resources. *Limnol. Oceanogr.* **36**, 1701–1714.
- Riebesell U., Burkhardt S., Dauelsberg A., and Kroon B. Carbon isotope fractionation by a marine diatom: Dependence on the growth rate limiting resource. *Mar. Ecol. Prog. Ser.* (submitted).
- Riebesell U. and Wolf-Gladrow D. (1995) Growth limits on phytoplankton. *Nature* **373**, 28.
- Riebesell U., Wolf-Gladrow D. A., and Smetacek V. (1993) Carbon dioxide limitation of marine phytoplankton growth rates. *Nature* **361**, 249–251.
- Roeske C. A. and O'Leary M. H. (1984) Carbon isotope effects on the enzyme-catalyzed carboxylation of ribulose biphosphate. *Biochemistry* **23**, 6275–6284.
- Roeske C. A. and O'Leary M. H. (1985) Carbon isotope effect on carboxylation of ribulose biphosphate catalyzed by ribulosebiphosphate carboxylase from *Rhodospirillum rubrum*. *Biochemistry* **24**, 1603–1607.
- Rotatore C., Colman B., and Kuzma M. (1995) The active uptake of carbon dioxide by the marine diatoms *Phaeodactylum tricornutum* and *Cyclotella* sp. *Plant Cell Environ.* **18**, 913–918.
- Round F. E., Crawford R. M., and Mann D. G. (1990) *The diatoms. Biology and morphology of the genera*. Cambridge University Press.
- Sackett W. M., Eckelmann W. R., Bender M. L., and Bé A. W. H. (1965) Temperature dependence of carbon isotope composition in marine plankton and sediments. *Science* **148**, 235–237.
- Salon C., Mir N. A., and Canvin D. T. (1996) HCO_3^- and CO_2 leakage from *Synechococcus* UTEX 625. *Plant Cell Environ.* **19**, 260–274.
- Sharkey T. D. and Berry J. A. (1985) Carbon isotope fractionation of algae as influenced by an inducible CO_2 concentrating mechanism. In *Inorganic Carbon Uptake by Aquatic Photosynthetic Organisms* (eds. W. J. Lucas and J. A. Berry), pp. 389–401. Am. Soc. Plant. Phys.
- Sültemeyer D., Biehler K., and Fock H. P. (1993) Evidence for the contribution of pseudocyclic photophosphorylation to the energy requirement of the mechanism for concentrating inorganic carbon in *Chlamydomonas*. *Planta* **189**, 235–242.
- Van den Hoek C., Mann D. G., and Jahns H. M. (1995) *Algae: An introduction to phycology*. Cambridge University Press.
- Whitney S. M. and Yellowlees D. (1995) Preliminary investigations into the structure and activity of ribulose biphosphate carboxylase from two photosynthetic dinoflagellates. *J. Phycol.* **31**, 138–146.
- Wolf-Gladrow D. and Riebesell U. (1997) Diffusion and reactions in the vicinity of plankton: A refined model for inorganic carbon transport. *Mar. Chem.* **59**, 17–34.